 Nucleic Acids Research, 1999, Vol. 27, No. 18 **3667–3675**

An NMR and mutational analysis of an RNA pseudoknot of *Escherichia coli* tmRNA involved in *trans*-translation

Nobukazu Nameki[1,2], Pratima Chattopadhyay[1], Hyouta Himeno[2,3], Akira Muto[2,3] and Gota Kawai[1,*]

[1]Department of Industrial Chemistry, Chiba Institute of Technology, Chiba 275-8588, Japan, [2]Department of Biology, Faculty of Science, Hirosaki University, Hirosaki 036-8561, Japan and [3]Department of Biochemistry and Biotechnology, Faculty of Agriculture and Life Science, Hirosaki University, Hirosaki 036-8561, Japan

Received June 7, 1999; Revised and Accepted July 27, 1999

ABSTRACT

Transfer-messenger RNA (tmRNA) is a unique molecule that combines properties from both tRNA and mRNA, and facilitates a novel translation reaction termed *trans*-translation. According to phylogenetic sequence analysis among various bacteria and chemical probing analysis, the secondary structure of the 350–400 nt RNA is commonly characterized by a tRNA-like structure, and four pseudoknots with different sizes. A mutational analysis using a number of *Escherichia coli* tmRNA variants as well as a chemical probing analysis has recently demonstrated not only the presence of the smallest pseudoknot, PK1, upstream of the internal coding region, but also its direct implication in *trans*-translation. Here, NMR methods were used to investigate the structure of the 31 nt pseudoknot PK1 and its 11 mutants in which nucleotide substitutions are introduced into each of two stems or the linking loops. NMR results provide evidence that the PK1 RNA is folded into a pseudoknot structure in the presence of Mg^{2+}. Imino proton resonances were observed consistent with formation of two helical stem regions and these stems stacked to each other as often seen in pseudoknot structures, in spite of the existence of three intervening nucleotides, loop 3, between the stems. Structural instability of the pseudoknot structure, even in the presence of Mg^{2+}, was found in the PK1 mutants except in the loop 3 mutants which still maintained the pseudoknot folding. These results together with their biological activities indicate that *trans*-translation requires the pseudoknot structure stabilized by Mg^{2+} and specific residues G61 and G62 in loop 3.

INTRODUCTION

Transfer-messenger RNA (tmRNA), a stable RNA molecule consisting of 350–400 nt, is found in many bacteria (1). The tmRNA was first found to be alanylated by alanyl-tRNA synthetase *in vitro* (2,3). In fact, it possesses a tRNA-like structure composed of a TΨC arm and an acceptor stem leading to the universal 3'-CCA. The acceptor stem possesses identity elements of $tRNA^{Ala}$ including a G-U pair at the third base pair position (4,5). The presence of tRNA-specific modified nucleosides has also been verified in the TΨC-loop of *Escherichia coli* tmRNA (6). Another property of tmRNA is that it adds a peptide tag to abnormal polypeptides due to incomplete mRNAs lacking a stop codon (7,8). This peptide tag, AlaAlaAsnAspGluAsnTyrAla-LeuAlaAla, was first found for mouse interleukin-6 expressed in *E.coli* (9) and subsequently it has also been found to be a signal for cellular cytoplasmic or periplasmic proteases that degrade the abnormal polypeptide (7). These observations of both tRNA and mRNA properties of the RNA molecule led to a model of a new translation mechanism termed '*trans*-translation', where the tmRNA recycles the ribosome that is stalled during translation due to the truncated mRNA lacking a stop codon (10). The tmRNA is aminoacylated with alanine by AlaRS and the alanyl-tmRNA enters the A-site of the stalled ribosome. After the peptidyl transfer of the nascent peptides to the tmRNA-bound alanine, the ribosome decodes the coding region in the tmRNA itself to add the rest of the tag peptide. It should be noted that the tmRNA binds predominantly to 70S ribosome and only a very small extent to polysome (11,12) probably indicating that the tmRNA does not bind to normally functioning ribosomes.

Secondary structure models of tmRNA that would be conserved among various bacteria were proposed by an extensive sequence alignment analysis (13), and a chemical and enzymatic probing analysis with a phylogenetic analysis (14). Additional probing data using a nickel complex cleaving U in folded RNA refined the model (15). The structure is characterized by not only a tRNA-like structure, but also by four pseudoknots, in which more than half the nucleotides are involved (Fig. 1). Among the four putative pseudoknots, the shortest one, PK1, is located upstream of the internal coding region.

Mutational analysis *in vitro* using a number of tmRNA variants as well as chemical probing analysis has demonstrated not only the presence of the PK1 structure but also its direct implication in *trans*-translation (16). Mutations disrupting each stem of PK1

*To whom correspondence should be addressed. Tel: +81 47 478 0425; Fax: +81 47 478 0425; Email: gkawai@ic.it-chiba.ac.jp
Present address:
Nobukazu Nameki, Faculty of Bioscience and Biotechnology, Tokyo Institute of Technology, Kanagawa 226-8501, Japan

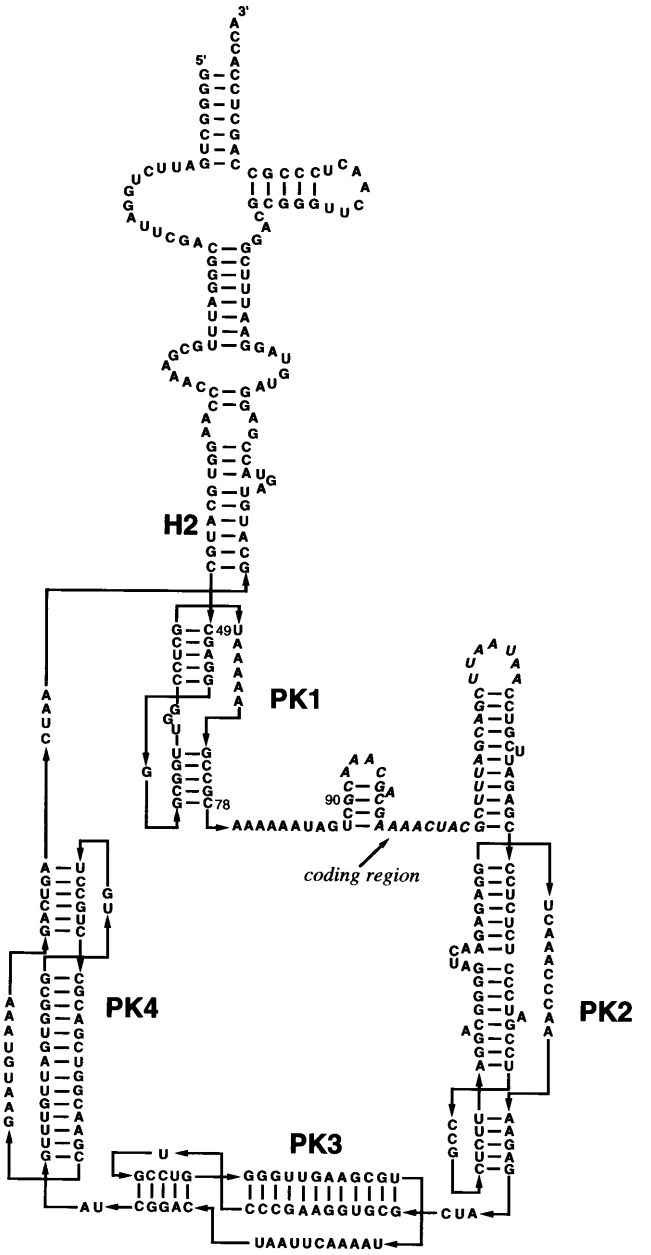

Figure 1. Possible secondary structure of tmRNA from *E.coli*. The internal coding region is indicated in italics. The pseudoknot structure PK1 is located upstream of the coding region.

inactivate both of the aminoacylation and alanine incorporation activities of tmRNA. The loop consisting of three nucleotides between the two stems is required for efficient *trans*-translation and the presence of Mg^{2+}(s) interacting with the loop has been suggested by the probing data. Although melting analysis and chemical probing analysis have been applied for some mutant tmRNAs, structural features of PK1 and its mutants are not clear yet.

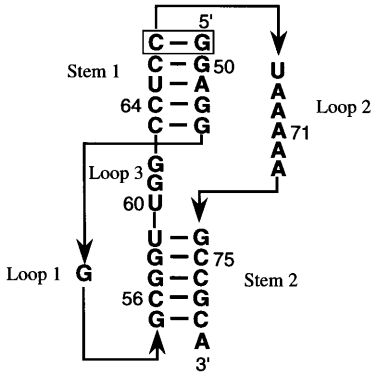

Figure 2. The nucleotide sequence of PK1 RNA used in the present study. Different notations of loop 2 and loop 3 from the previous work (16) were used to compare our results with previous structural works.

In the present study, NMR methods were used to investigate the structures of the 31 nt pseudoknot, PK1 (Fig. 2), and its 11 mutants as shown in Table 1. Since most of the corresponding tmRNA mutants were examined for the aminoacylation and alanine incorporation activities *in vitro*, correlation between structures of the PK1 mutants and the biological activities of the corresponding tmRNA mutants is discussed.

MATERIALS AND METHODS

RNA synthesis and purification

All RNAs were synthesized using an automatic DNA/RNA synthesizer, Expedite Model 8909 (PerSeptive Biosystem, Inc., MA, USA). After deprotection with ammonia and tetra-*n*-butylammonium fluoride, RNAs were purified by 20% PAGE under denaturing conditions with 7 M urea. The RNAs were eluted from the gel in water and were desalted by a C18 cartridge, Sep-Pack Plus (Waters, MA, USA), and were evaporated to dryness.

NMR experiments

The purified RNA was incubated for 5 min at 95°C, and then cooled with ice. Samples typically contained 0.3–0.6 mM RNA dissolved in 200 µl of 10 mM sodium phosphate buffer in the absence or presence of 5 mM Mg^{2+} in 90% H_2O/10% D_2O at pH 6.8. NMR spectra were measured on a DRX-500 or DRX-600 spectrometer (Bruker) at 15 or 25°C with symmetrical NMR microtubes (Shigemi Co. Ltd, Japan). Solvent signal was suppressed by the jump-and-return pulse (17) for all experiments with pulse intervals of 65 µs for 500 MHz and 59 µs for 600 MHz. For all one-dimensional measurements, spectral width of 25 p.p.m. and data points of 32 K were used, and the number of scans was 400–800. Prior to Fourier transformation, line broadening of 3 Hz was applied. Two-dimensional NOESY experiments (18) were observed with a mixing time of 150 ms. 512 FIDs of 2 K were collected with the States-TPPI methods (18), and the number of scans was 96–400. Prior to Fourier transformation, $\pi/2$-shifted squared sinebell function

Table 1. Nucleotide sequences of PK1 mutants and relative activities of their corresponding tmRNA mutants

Mutant	Sequence	Alanine incorporation	Aminoacylation
	S1 L2 5'GGAGG G GCGGU UGG CCUCC UAAAAA GCCGC A 3' L1 L3 S2 50 60 70 80		
49G67C[1]		1.10 (0.20)	1.51 (0.21)
50CUC	-CUC- - ----- --- ----- ------ ----- -	0.12 (0.05)	0.45 (0.09)
50CUC-64GAG	-CUC- - ----- --- -GAG- ------ ----- -	0.78 (0.15)	0.73 (0.12)
56GCC	----- - -GCC- --- ----- ------ ----- -	0.60 (0.13)	0.67 (0.12)
56GCC-75GGC	----- - -GCC- --- ----- ------ -GGC- -	1.00 (0.18)	0.43 (0.09)
60C	----- - ----- C-- ----- ------ ----- -	1.03 (0.19)	0.77 (0.13)
61C	----- - ----- -C- ----- ------ ----- -	0.67 (0.14)	1.09 (0.17)
62C	----- - ----- --C ----- ------ ----- -	0.43 (0.10)	1.10 (0.17)
61UU	----- - ----- -UU ----- ------ ----- -	0.36 (0.09)	0.83 (0.14)
6162del	----- - ----- -** ----- ------ ----- -	—	—
606162del[2]	----- - ----- *** ----- ------ ----- -	0.40 (0.10)	1.06 (0.16)
71CC[1]	----- - ----- --- ----- ---CC- ----- -	0.20 (0.07)	0.28 (0.04)
71GG	----- - ----- --- ----- ---GG- ----- -	—	—
69UU71GG[2]	----- - ----- --- ----- -UUGG- ----- -	0.69 (0.14)	0.67 (0.12)

The nucleotides that have been mutated are shown explicitly and the unchanged ones are indicated by short bars. Asterisks correspond to nucleotide deletions. Relative activities to the wild-type tmRNA are shown from ref. 16, obtained *in vitro* using tmRNA mutants with C49-G67, except for the G49-C67 mutant. Alanine incorporation to the tag sequence is used as *trans*-translation activity. Standard deviations are indicated in parentheses.

[1]Activities of 49G67C and 71CC were measured in this study under the same conditions as those used by Nameki *et al.* (16).

[2]NMR measurements of these PK1 mutants were not performed.

for t2 dimension and π/2-shifted sinebell function for t1 dimension were applied and zero-filling was applied to obtain 2×1 K^2 real spectra.

RESULTS AND DISCUSSION

Design of PK1

The 31 nt RNA, PK1 (Fig. 2), was constructed by chemical synthesis, as well as the 11 mutants (Table 1). Different notations of loop 2 and loop 3 from the previous work (16) were used to compare our results to previous structural works. Considering preparation using the *in vitro* transcription system, we modified the stem 1 sequence without changing its nucleotide composition: the first base pair, C49-G67, in stem 1 was changed to G49-C67 so that transcription starts with a guanosine residue. We confirmed that the tmRNA mutant with the modified sequence of G49-C67 has almost identical aminoacylation and alanine incorporation activities to those of the wild-type (Table 1). Besides, we added an adenosine residue to the 3' end of PK1 to stabilize the terminal base pair of the stem. All the mutations were introduced to this modified sequence of PK1.

Assignments of the imino proton resonances of PK1

Figure 3 shows the imino proton region of the 600 MHz ^{1}H-NMR spectra of PK1 at 15 (a) and 25°C (b) in the presence of 5 mM Mg^{2+}. Considering resonances overlapping at 13.65 (a) and 12.5 p.p.m. (b), 11 imino proton resonances were observed and this is consistent with the predicted secondary structure as shown in Figure 2. Judging from the chemical shift, the signal observed at 14.6 p.p.m. (a) was tentatively assigned to an imino proton in an A-U pair and signals at 11.4 and 11.25 p.p.m. (a) were possibly due to imino protons in a G-U pair. The former was confirmed by the presence of typical NOE crosspeaks between the imino proton of U and the H2 proton of A in an A-U pair (data not shown). The latter was also confirmed by strong NOE crosspeaks between the two imino protons in a G-U pair (Fig. 4).

Figure 4 shows the sequential assignment of the imino proton resonances. Starting at the resonance at 12.7 p.p.m., all resonances except the resonance at 12.95 p.p.m. can be connected via NOE crosspeaks, resulting in unambiguous resonance assignments as G50-U65-G52-G53-U59/G74-G58-G57-G77-G55.

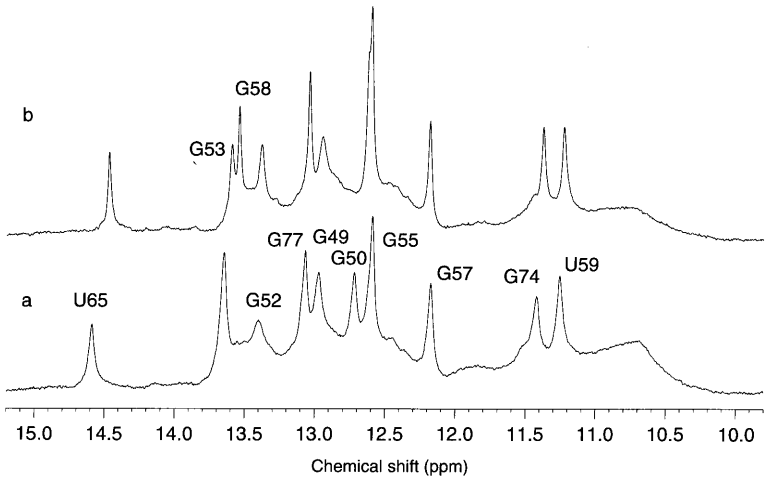

Figure 3. Imino proton region of the 600-MHz ^{1}H-NMR spectra of PK1. The spectra were recorded at 15°C (**a**) and at 25°C (**b**) in 5% D_2O, 10 mM phosphate buffer (pH 6.8) and 5 mM $MgCl_2$. Resonance assignments are indicated in the spectrum at 15°C except for G53 and G58 which are overlapped at this temperature.

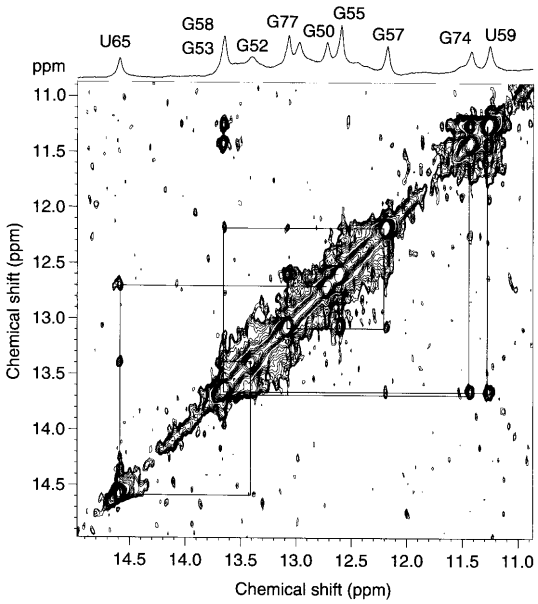

Figure 4. Imino proton region of the 2D NOESY spectrum recorded at 15°C. The mixing time was 150 ms. Sequential NOE connectivity is indicated.

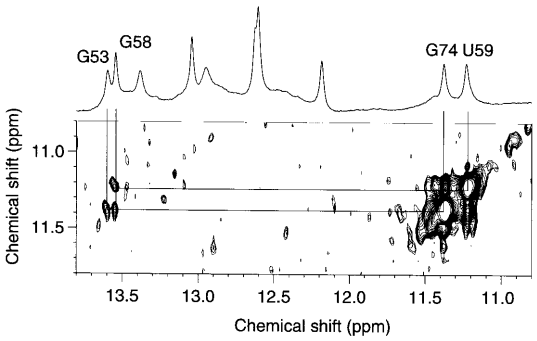

Figure 5. A part of the 2D NOESY spectrum recorded at 25°C and corresponding 1D spectrum. The mixing time was 150 ms.

The NOESY spectrum at 25°C was helpful to confirm the NOE walk around the overlapping resonances at 15°C (Fig. 5). Assignments of U59 and G74 were confirmed with the ^{15}N-^{1}H HMQC spectrum of ^{15}N/^{13}C-labeled PK1 sample which was prepared by the *in vitro* transcription system (to be published). The resonance at 12.95 p.p.m. was then assigned to G49 and this was confirmed by the comparison of the spectrum of PK1 with C49-G67 and PK1 with G49-C67 (data not shown). The results of resonance assignments are shown in Figure 3.

A pseudoknot conformation of PK1

As described above, an NOE between G53 and G74 was observed as well as NOEs between G58 and G74/U59 as shown in Figure 5, indicating that stem 1 and stem 2 are stacked to each other. Thus, it was found that PK1 RNA is folded into a pseudoknot structure, as suggested by phylogenetic sequence alignments and a chemical probing analysis (13–16). Imino proton resonances were observed consistent with formation of two helical stem regions, where stem 1 contains 5 bp, and stem 2 has 5 bp including a G-U pair. Probing data that use the entire tmRNA argue against a standard A51-U65 Watson–Crick base pair in stem 1, and favor an internal bulge A51··U65.

However, in this study using only an PK1 sequence fragment, formation of a Watson–Crick type A51-U65 pair is obvious.

Pseudoknot was one of the RNA structures that have been well investigated by NMR. Most of the NMR results have indicated that the two stems of pseudoknot typically stack to each other forming a coaxial helix (19–21) and this is also applicable to the results for PK1 as described above. However, NMR analysis of pseudoknots found in mouse mammary tumor virus RNA has revealed a characteristic bent conformation of the RNA pseudoknot that promotes frameshifting during translation (22). In this case, a single adenosine residue at the junction of its two stems is intercalated between the stems so that direct coaxial stacking of the stems is not possible. As for PK1, judging from the NMR results, three residues at the junction of its two stems bulge out from the continuous stems to make a characteristic pseudoknot conformation. Another characteristic is that loop 1 consists of a single guanosine residue. A single-nucleotide loop 1 has also been found in a pseudoknot within the gene 32 mRNA of bacteriophage T2 and NMR analysis has shown that 6 or 7 bp in stem 2 are required for this type of pseudoknot formation (23). In the case of PK1, Mg^{2+} may play an important role in forming the pseudoknot conformation even with a single residue in loop 1 and 5 bp in stem 2 as described below.

Requirement of Mg^{2+} for a stable pseudoknot conformation

Figure 6 shows the imino proton spectra of PK1 (0.5 mM) over a Mg^{2+} concentration range of 0–10 mM. In the absence of Mg^{2+}, all the resonances significantly broadened. In particular, neither resonance of the U65 in stem 1 nor the resonances of the U59-G74 in stem 2 were observed, indicating the conformational instability of the pseudoknot in the absence of Mg^{2+}. In contrast, in the presence of equimolar concentrations (0.5 mM) of Mg^{2+}, the spectrum changed drastically to that of PK1 in the pseudoknot conformation, indicating that PK1 binds a single Mg^{2+} to fold into the pseudoknot conformation. Between 1 and 5 mM Mg^{2+} only two signals, corresponding to G77 and G50, shifted slightly and no significant changes in the spectra were observed for Mg^{2+} concentration of >5 mM.

These results indicate that a single Mg^{2+} molecule stabilizes both stems 1 and 2 to form a continuous helix. Probably, the Mg^{2+} binds to the joint region including loop 3 and this is consistent with the previous probing data suggesting that Mg^{2+}(s) bind around loop 3 of the PK1 region in tmRNA (16). In this respect, the structure of this 31 nt PK1 appears to be the same situation as that of the PK1 region in tmRNA. It should be noted that an attempt to remove the bound Mg^{2+} by ultrafiltration with 5 mM EDTA did not change the imino proton spectrum (data not shown), indicating that the Mg^{2+} binding is quite strong.

Conformation of mutants and its relation to the biological activities

We have previously constructed a number of tmRNA mutants focused upon the PK1 region, and examined their biological activities *in vitro* (16). Here, structures of the corresponding 11 mutants of PK1 as shown in Table 1 were investigated by NMR. It should be noted that each mutant PK1 RNA sample prepared for NMR measurements behaved as a monomer in the denatured PAGE except for 50CUC-64GAG which gave a minor band corresponding to a dimer (data not shown). To confirm the formation of G-U base pairs, NOESY spectra were

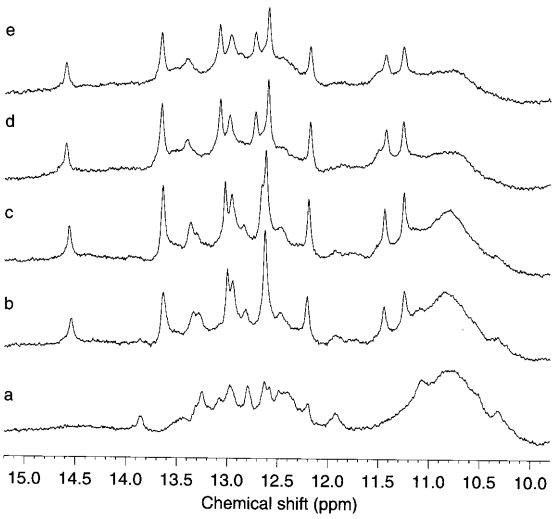

Figure 6. Mg^{2+} dependence of imino proton resonances at 500 MHz. The sample concentration was 0.5 mM and Mg^{2+} concentrations were (**a**) 0 mM, (**b**) 0.5 mM, (**c**) 1 mM, (**d**) 5 mM and (**e**) 10 mM. Measurements were made at 15°C.

measured for mutants which gave sharp imino proton resonances. Table 1 also shows the relative activity for alanine incorporation to the tag sequence as the *trans*-translation activity and aminoacylation to its 3'-adenosine residue (16), obtained *in vitro* using tmRNA mutants with C49-G67, except for the G49-C67 mutant.

Figure 7 shows the NMR spectra of the mutants of stem 1 and stem 2 in the absence (a) and presence (b) of Mg^{2+}. 50CUC mutation was designed to disrupt stem 1 and 50CUC-64GAG was its compensatory mutant. The tmRNA mutant with 50CUC mutation is one of the worst substrates for both the aminoacylation and alanine incorporation activities among all variants tested (16). In the absence of Mg^{2+}, more than seven imino proton resonances were observed, including those due to a G-U pair as indicated in the figure. The spectrum is different from that of the PK1 pseudoknot structure and chemical shifts for the observed G-U resonances are significantly different from those for the PK1 G74-U59 base pair. Thus, it is likely that this mutant forms an alternative secondary structure. Figure 8a shows a possible secondary structure for the mutant. In the presence of Mg^{2+}, the resonances broadened but showed a similar pattern, indicating that this mutant still prefers the alternative conformation. This is consistent with the fact that, according to the altered UV melting profile together with chemical probing data, the corresponding tmRNA mutant has an alternative conformation that is more stable than that of wild-type tmRNA. Thus, it is suggested that the poor biological activities of this tmRNA mutant are due to the conformational change of the PK1 region. The compensatory mutation for 50CUC, 50CUC-64GAG, was designed to restore stem 1, but the spectra of PK1 with 50CUC-64GAG are similar to those of PK1 with 50CUC mutation, indicating that the alternative conformation is more stable than the pseudoknot conformation. The NOE pattern in the NOESY spectra for 50CUC and

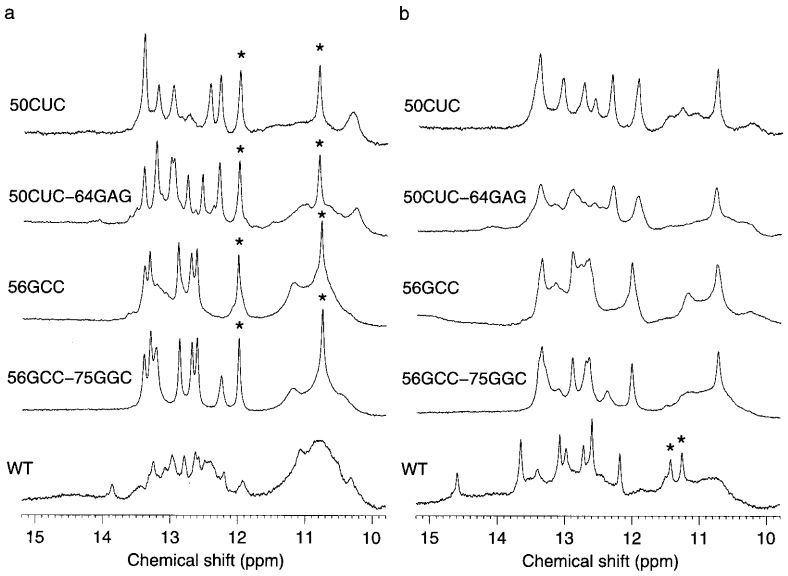

Figure 7. The imino proton spectra of mutants of stems 1 and 2, in the absence (**a**) and presence (**b**) of 5 mM Mg^{2+} at 500 MHz. Each spectrum was recorded at 15°C in 10 mM phosphate buffer (pH 6.8). Resonances due to G-U pairs confirmed by NOESY experiments are indicated by asterisks (*).

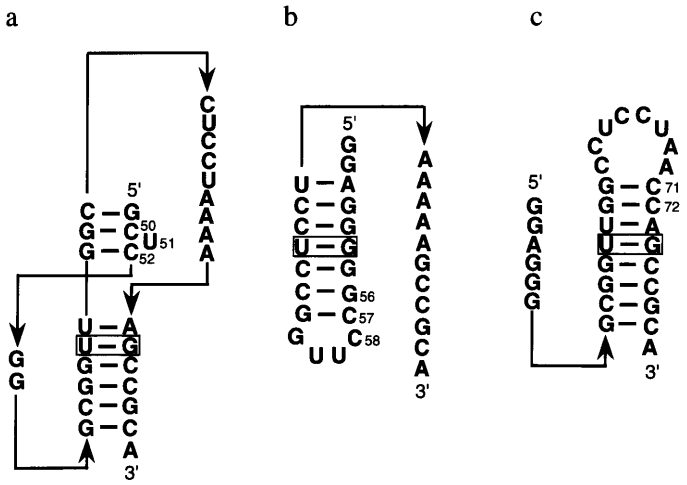

Figure 8. Possible secondary structures of mutants: (**a**) 50CUC, (**b**) 56GCC and (**c**) 71CC. Mutated residues are numbered and G-U pairs are indicated by boxes.

50CUC-64GAG in the absence of Mg^{2+} is also similar and is essentially consistent with the possible secondary structure shown in Figure 8a (data not shown). However, the tmRNA mutant with 50CUC-64GAG shows a UV melting profile similar to wild-type but not to the mutant with 50CUC (16). This well reflects their biological activities, and thus pseudoknot conformation may be recovered in the tmRNA compensatory mutant.

The mutation in stem 2, 56GCC, also showed different spectra compared with wild-type PK1. Again, resonances due to a G-U pair were observed. This also indicates the formation of an alternative conformation. In this case, the G74-U59 pair cannot form for this mutant because the adjacent base pairs were disrupted. Figure 8b shows a possible secondary structure of this mutant in which the G54-U65 pair is formed. Thus, this again suggests that the formation of an alternative conformation in the PK1 region decreases the biological activity of tmRNA. The spectra as well as the NOE pattern in the NOESY spectra for the compensatory mutant, 56GCC-75GGC, were also similar to those of 56GCC (data not shown), indicating the existence of the alternative conformation even in the compensatory

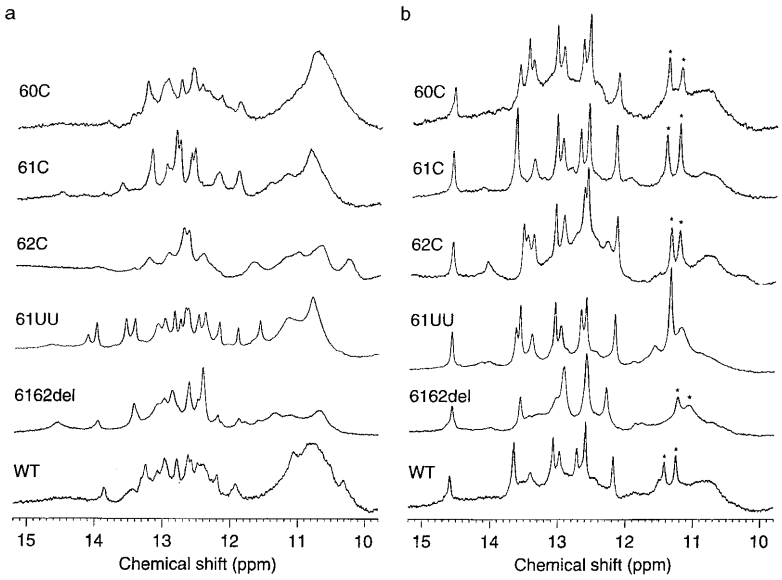

Figure 9. The imino proton spectra of mutants of loop 3, in the absence (**a**) and presence (**b**) of 5 mM Mg^{2+} at 500 MHz. Each spectrum was recorded at 15°C in 10 mM phosphate buffer (pH 6.8). Resonances due to G-U pairs confirmed by NOESY experiments are indicated by asterisks (*).

mutant. Because the 56GCC-75GGC mutant recovers the alanine incorporation activity, the pseudoknot conformation may be preferred in the corresponding tmRNA as is the case for the tmRNA with 50CUC-64GAG.

One of the characteristics of PK1 is loop 3 consisting of three nucleotides between the two stems. Figure 9 shows the imino proton spectra of mutants for loop 3. Base substitution at each of three nucleotides, 60C, 61C and 62C, did not affect the imino proton spectra in the presence of Mg^{2+}, although the spectra in the absence of Mg^{2+} showed some difference. This indicates that the sequence of loop 3 is not essential for the pseudoknot formation. Furthermore, PK1 mutants having substitution or deletion of the two nucleotides at positions 61 and 62 also gave characteristic spectra for the pseudoknot conformation. For PK1 with a 61UU mutation, the signals due to G74-U59 are overlapped. NOESY spectra for these five mutants also gave the characteristic pattern for the pseudoknot conformation in the presence of Mg^{2+} (data not shown). Thus, loop 3 is not essential for pseudoknot formation. In fact, the aminoacylation activity of tmRNA was not affected by mutations in loop 3. The activity reduction for alanine incorporation caused by nucleotide change at G61 and/or G62 would be due to inhibition of direct interaction with ribosome or other possible factors involved in *trans*-translation function, or with other structural domains of tmRNA.

Since Mg^{2+} is required for the pseudoknot formation for all the loop 3 mutants described above, the bases in loop 3 are not directly involved in Mg^{2+} binding, unlike the G-G metal ion binding site as described recently for a 5S rRNA domain solved by X-ray crystallography (24).

Originally, the 61UU mutant was designed so that the changed nucleotides in loop 3 could form base pairs with nucleotides in loop 2, thus creating three successive A-U pairs as a part of the extended stem 2. Imino proton spectrum of PK1 with 61UU in the absence of Mg^{2+} probably indicates the formation of the aimed A-U pairs. However, upon addition of Mg^{2+}, the mutant PK1 formed an almost normal pseudoknot conformation as shown in Figure 9.

The 71CC mutant was designed so that the nucleotides of loop 3 could form base pairs with the substituted nucleotide of loop 2. The imino proton spectra of PK1 with 71CC were completely different from that of wild-type PK1 and indicated the formation of an alternative secondary structure with a U59-G74 pair as shown in Figure 8c. NMR studies using 26 nt oligonucleotides have demonstrated that appropriate size and sequence of loop 2 are required for the stable pseudoknot structure (25) and this is probably the reason why the mutant does not form a pseudoknot even though the sequence of stem 1 is intact. The preference of the alternative structure of the 71CC mutant as shown in Figure 10 may probably cause the low biological activity of the corresponding tmRNA mutant.

The 71GG mutant gave a similar spectrum to that of the wild-type in the absence of Mg^{2+}. However, this mutant did not give a typical spectrum of pseudoknot in the presence of Mg^{2+} and the tmRNA mutant with 69UU71GG shows partial biological activity. Thus, it is suggested that A71 and A72 are required for Mg^{2+}-dependent stable pseudoknot formation. It is possible that A71 and/or A72 are the sites of the strong Mg^{2+} binding and this causes the difference in stability of the pseudoknot conformation between 61UU and 71CC mutants. Detailed NMR structure of a pseudoknot from plant viral genomic RNA showed the intricate interactions related to the loops of the pseudoknot (20). Loop 2, which crosses the major groove of stem 1, interacts closely with its opposing helix, in particular through hydrogen bonds with a highly conserved adenosine in

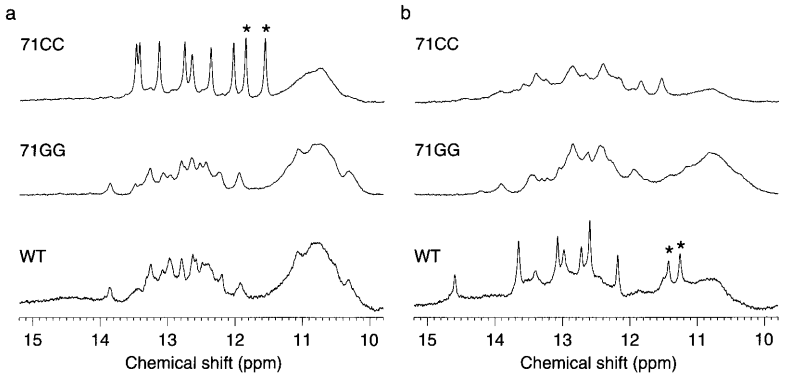

Figure 10. The imino proton spectra of mutants of loop 2, in the absence (**a**) and presence (**b**) of 5 mM Mg^{2+} at 500 MHz. Each spectrum was recorded at 15°C in 10 mM phosphate buffer (pH 6.8). Resonances due to G-U pairs confirmed by NOESY experiments are indicated by asterisks (*).

loop 2 (20). A similar interaction is also the candidate for the structural stabilization in the PK1 pseudoknot.

Structural features of PK1 in tmRNA

The NMR results demonstrated that the PK1 RNA folds into a Mg^{2+}-dependent pseudoknot structure, in which the two stems stack to each other in spite of three intervening residues between the two stems. NMR spectra of the PK1 mutants for stems 1 and 2 revealed structural instability of the mutants even in the presence of Mg^{2+}. This destabilization of those mutants indicates that the PK1 is well designed to form a stable pseudoknot in the presence of Mg^{2+}. On the other hand, the mutants in loop 3 were still found to form the Mg^{2+}-dependent pseudoknot in spite of the biological inactivity of the corresponding tmRNA mutants. In conclusion, our results indicate that efficient *trans*-translation reaction of tmRNA requires the PK1 region to be a stable pseudoknot conformation with G61G62 in loop 3.

As for other pseudoknots in tmRNA, probing analysis using a nickel complex toward chemically synthesized RNA has shown that the folding of the PK4 pseudoknot is also Mg^{2+} dependent (15). In the absence of Mg^{2+}, PK4 is an open conformation as a hairpin with stem 1. Mg^{2+} dependence of the UV melting has suggested that the tertiary structure of *E.coli* tmRNA nucleates around a Mg^{2+} core, as shown for the P4-P6 domain of the *Tetrahymena* group I intron (26). Thus, Mg^{2+} seems to be a key factor for the stabilization of not only each structural unit of tmRNA, but also the total tmRNA.

A pseudoknot often plays a key role in translational processes, for example in 16S rRNA (27), programmed frameshifting in decoding many viruses (28–30) and mammalian ornithine decarboxylase antizyme (31). Now a novel pseudoknot conformation is found in this study and this PK1 pseudoknot is added to the list of pseudoknots involved in translation.

Further functional and structural studies of PKs 2, 3 and 4 as well as PK1 are necessary to reveal the structure–function relationships of tmRNA. Accumulation of structural information of each domain of tmRNA, as well as phylogenetic analyses (32–34), will lead us to the 3D structure of the whole tmRNA molecule.

ACKNOWLEDGEMENTS

We are indebted to Prof. N. Okada of the Tokyo Institute of Technology for critical comments. We also thank Drs K. Hosono, A. Takasu, T. Sakamoto and K. Takahashi for their help and advice for NMR analysis, Miss H. Shirakura for her assistance in NMR sample preparation, and Drs K. Hanawa and M. Ishii for helpful assistance in preparation of tmRNA variants. Gratitude is extended to the Gene Research Center of Hirosaki University. This work was supported by 'Research for the Future' Program (JSPS-RFTF97L00503) from the Japan Society for the Promotion of Science and, in part, by a Grants-in-aid for High Technology Research and Scientific Research on Priority Areas from the Ministry of Education, Science, Sports and Culture, Japan.

REFERENCES

1. Muto,A., Sato,M., Tadaki,T., Fukushima,M., Ushida,C. and Himeno,H. (1996) *Biochimie*, **78**, 985–991.
2. Ushida,C., Himeno,H., Watanabe,T. and Muto,A. (1994) *Nucleic Acids Res.*, **22**, 3392–3396.
3. Komine,Y., Kitabatake,M., Yokogawa,T., Nishikawa,K. and Inokuchi,H. (1994) *Proc. Natl Acad. Sci. USA*, **91**, 9223–9227.
4. McClain,W.H. and Foss,K. (1988) *Science*, **240**, 793–796.
5. Hou,Y.-M. and Schimmel,P. (1988) *Nature*, **333**, 140–145.
6. Felden,B., Hanawa,K., Atkins,J.F., Himeno,H., Muto,A., Gesteland,R.F., McCloskey,J.A. and Crain,P.F. (1998) *EMBO J.*, **17**, 3188–3196.
7. Keiler,K.C., Waller,P.R.H. and Sauer,R.T. (1996) *Science*, **271**, 990–993.
8. Himeno,H., Sato,M., Tadaki,T., Fukushima,M., Ushida,C. and Muto,A. (1997) *J. Mol. Biol.*, **268**, 803–808.
9. Tu,G.F., Reid,G.E., Zhang,J.-G., Moritz,R.L. and Simpson,R.J. (1995) *J. Biol. Chem.*, **270**, 9322–9326.
10. Muto,A., Ushida,C. and Himeno,H. (1998) *Trends Biochem. Sci.*, **23**, 25–29.
11. Ushida,C., Himeno,H., Watanabe,T. and Muto,A. (1994) *Nucleic Acids Res.*, **22**, 3392–3396.
12. Tadaki,T., Fukushima,M., Ushida,C., Himeno,H. and Muto,A. (1996) *FEBS Lett.*, **399**, 223–226.
13. Williams,K.P. and Bartel,D.P. (1996) *RNA*, **2**, 1306–1310.

14. Felden,B., Himeno,H., Muto,A., McCutcheon,J.P., Atkins,J.F. and Gesteland,R.F. (1997) *RNA*, **3**, 89–103.
15. Hickerson,R.P., Watkins-Sims,C.D., Burrows,C.J., Atkins,J.F., Gesteland,R.F. and Felden,B. (1998) *J. Mol. Biol.*, **279**, 577–587.
16. Nameki,N., Felden,B., Atkins,J.F., Gesteland,R.F., Himeno,H. and Muto,A. (1999) *J. Mol. Biol.*, **286**, 733–744.
17. Plateau,P. and Gueron,M. (1982) *J. Am. Chem. Soc.*, **104**, 7310–7311.
18. Ernst,R.R., Bodenhausen,G. and Wokaun,A. (1987) *Principles of Nuclear Magnetic Resonance in One and Two Dimensions*. Oxford Science Publications,Oxford.
19. Puglisi,J.D., Wyatt,J.R. and Tinoco,I.,Jr (1990) *J. Mol. Biol.*, **214**, 437–453.
20. Kolk,M.H., van der Graaf,M., Wijmenga,S.S., Pleij,C.W.A., Heus,H.A. and Hilbers,C.W. (1998) *Science*, **280**, 434–438.
21. Holland,J.A., Hansen,M.R., Du,Z. and Hoffman,D.W. (1999) *RNA*, **5**, 257–271.
22. Chen,X.K., Shen,L.X., Chamorro,M., Varmus,H.E. and Tinoco,I.,Jr (1996) *J. Mol. Biol.*, **260**, 479–483
23. Du,Z. and Hoffman,D.W. (1997) *Nucleic Acids Res.*, **25**, 1130–1135.
24. Correll,C.C., Freeborn,B., Moore,P.B. and Steitz,T.A. (1997) *Cell*, **91**, 705–712.
25. Wyatt,J.R., Puglisi,J.D. and Tinoco,I.,Jr (1990) *J. Mol. Biol.*, **214**, 455–470.
26. Cate,J.H., Hanna,R.L. and Doudna,J.A. (1997) *Nature Struct. Biol.*, **4**, 553–558.
27. Powers,T. and Noller,H.F. (1991) *EMBO J.*, **10**, 2203–2214.
28. Brierley,I., Digard.P. and Inglis,S.C. (1989) *Cell*, **57**, 537–547.
29. ten Dam,E., Brierley,I., Inglis,S. and Pleij,C. (1994) *Nucleic Acids Res.*, **22**, 2304–2310.
30. Gesteland,R.F. and Atkins,J.F. (1996) *Annu. Rev. Biochem.*, **65**, 741–768.
31. Matsufuji,S., Matsufuji,T., Miyazaki,Y., Murakami,Y., Atkins,J.F., Gesteland,R.F. and Hayashi,S. (1995) *Cell*, **80**, 51–60.
32. Williams,K.P. (1999) *Nucleic Acids Res.*, **27**, 165–166.
33. Wower,J. and Zwieb,C. (1999) *Nucleic Acids Res.*, **27**, 167.
34. Zwieb,C., Wower,I. and Wower,J (1999) *Nucleic Acids Res.*, **27**, 2063–2071.